Figure S1

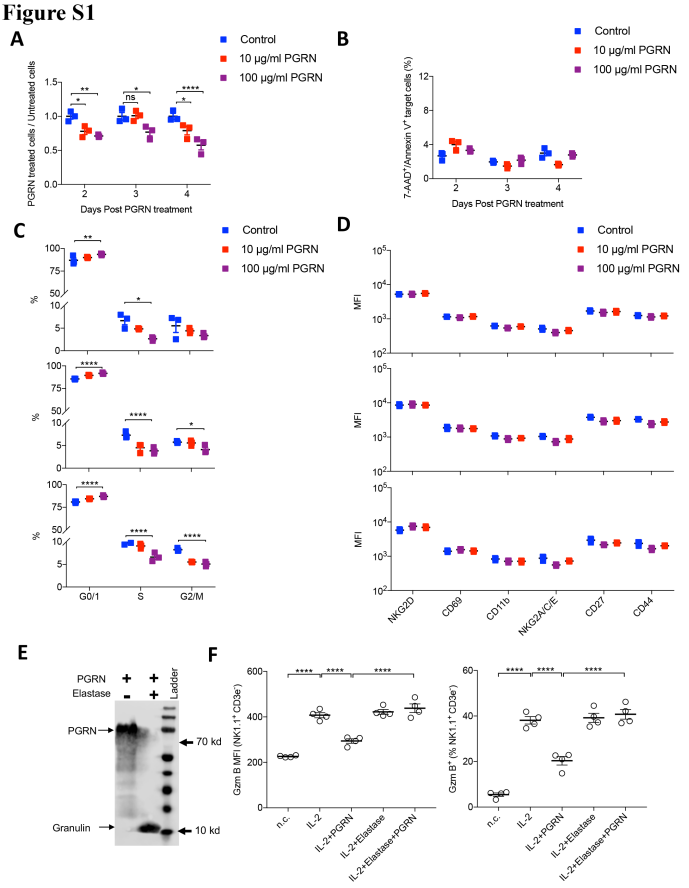

Supplementary Figure 1. Progranulin but not Granulin suppresses NK cell activation. (A-D) Freshly isolated NK cells were expanded with IL-2 and indicated doses of recombinant PGRN. The NK cell numbers **(A,** n=3**)**, NK cell viability **(B,** n=3**)**, NK cell cycle **(C,** n=3**)** and NK cell surface receptors **(D,** n=3**)** were measured at indicated time points. In (A), the graph illustrates a normalized value: (NK cell number in presence of PGRN) / (NK cell number in absence of PGRN). **(E and F)** PGRN proteins were incubated with Elastase (1.0 unit) for 24h. **(E)** The efficacy of PGRN digestion was confirmed by western blotting. **(F)** WT splenocytes were not stimulated (n.c.), stimulated with IL-2 (IL-2), IL-2 in presence of PGRN, IL-2 in presence of elastase, or IL-2 in presence of elastase digested PGRN, followed by Granzyme B staining (n=4). Data show mean ± s.e.m *$p < 0.05$, **$p < 0.001$, ***$p < 0.0002$, ****$p < 0.0001$.

Figure S2

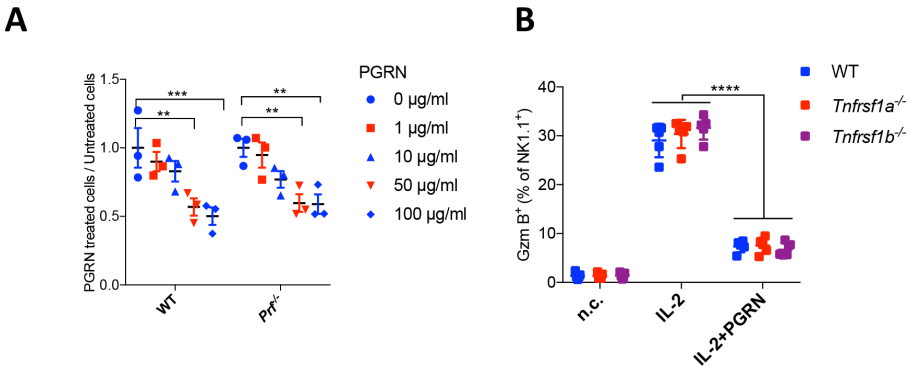

Supplementary Figure 2. The impact of PGRN on *Prf1*$^{-/-}$, *Tnfrsf1a*$^{-/-}$ and *Tnfrsf1b*$^{-/-}$ NK cells. (A) Freshly isolated NK cells from *Prf1*$^{-/-}$ spleen tissue was treated with IL-2 and different doses of PGRN for 4 days (n=3). The graphs illustrate a normalized value: (NK cell number in presence of PGRN) / (NK cell number in absence of PGRN). **(B)** Splenocytes from WT, *Tnfrsf1a*$^{-/-}$ and *Tnfrsf1b*$^{-/-}$ mice were stimulated with 1000U/ml IL-2 with or without PGRN for 6h. Granzyme B levels were measured by flow cytometry (n=5). Data show mean ± s.e.m. *$^{**}p < 0.001$, $^{***}p < 0.0002$, $^{****}p < 0.0001$.

Figure S3

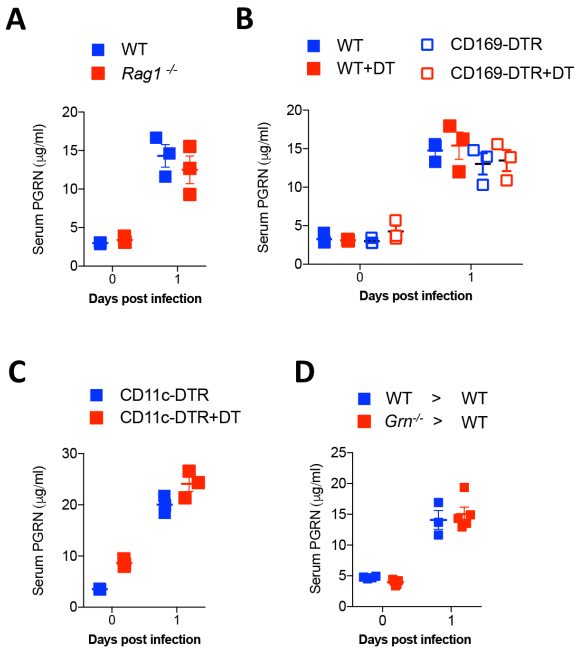

Supplementary Figure 3. T cells, B cells, CD169^{+} and CD11c^{+} cells are dispensable for PGRN expression during viral infection. (A) Wild type (WT) mice and *Rag1*$^{-/-}$ mice were infected with 2*10^{6} pfu WE (n=3). The serum PGRN protein levels were measured by ELISA at day 1 p.i.. **(B and C)** CD169-DTR and CD11c-DTR mice were treated with Diphtheria toxin (DT, 100 ng/mouse) at day -2 followed by infection with 2*10^{6} pfu LCMV-WE at day 0 (n=3). The serum PGRN protein levels were measured by ELISA at day 1 p.i. **(D)** Lethally irradiated control mice were reconstituted with control or *Grn*$^{-/-}$ bone marrow cells. Mice were infected with 2*10^{6} pfu LCMV WE and the serum PGRN levels were measured by ELISA (n=3-5). Data show mean ± s.e.m.

Figure S4

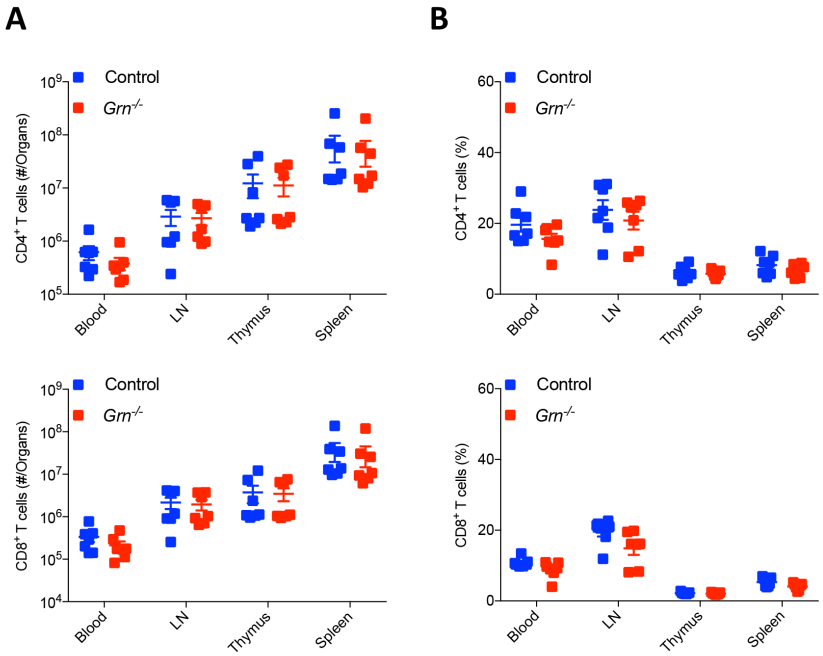

Supplementary Figure 4. Naïve *Grn*$^{-/-}$ mice exhibit no gross T cell phenotype. T cells were analysed in naïve *Grn*$^{-/-}$ and control mice. **(A)** CD4^{+} T cell number (*upper panel*) and CD8^{+} T cell number (*lower panel*) was measured in tissue harvested from control and *Grn*$^{-/-}$ mice as indicated (n=7 per group). **(B)** The frequency of CD4^{+} T cells (*upper panel*) and CD8^{+} T cells (*lower panel*) were determined in control and *Grn*$^{-/-}$ mice (n=7). Data show mean ± s.e.m. pooled from two experiments.

Figure S5

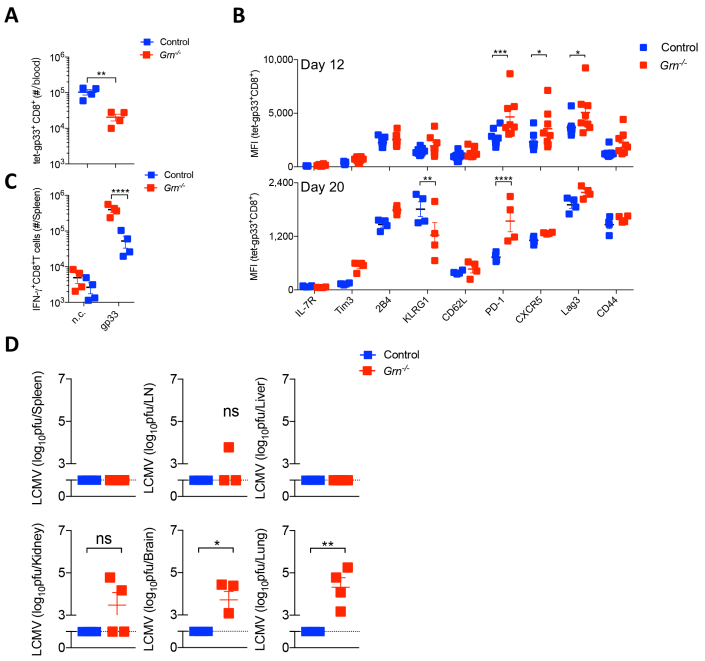

Supplementary Figure 5. *Grn*$^{-/-}$ mice have reduced anti-viral T cell immunity after LCMV infection. Control and *Grn*$^{-/-}$ mice were infected with 2*10^{6} LCMV-WE. **(A)** Absolute numbers of anti-viral CD8^{+} T cells from blood were measured by flow cytometry at day 20 (n=4). **(B)** Surface molecule expression on anti-viral CD8^{+} T cells from blood samples 12 (upper panel) or 20 (lower panel) days after infection were measured (n=4). **(C)** IFNγ^{+}CD8^{+} T cells were determined after re-stimulation with the LCMV epitopes gp33 and np396 at day 20 p.i. (n=4). **(D)** Virus titers were examined by plaque assays at day 20 p.i. (n=4). Data show mean ± s.e.m.; *$p < 0.05$, **$p < 0.001$, ****$p < 0.0001$.

Figure S6

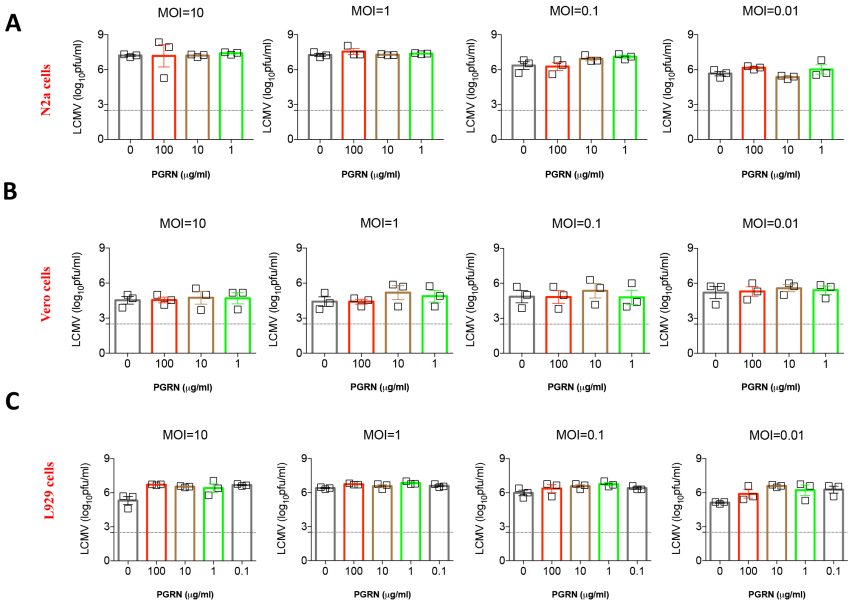

Supplementary Figure 6. LCMV replication remains intact in presence of PGRN. N2a neuroblastoma cells **(A,** n=3**)**, Vero **(B,** n=3**)** and L929 **(C,** n=3**)** cells were incubated with the indicated concentrations of PGRN protein. Subsequently, the cells were infected with the indicated doses of LCMV-WE. The replication of virus was determined by plaque assays. Data show mean ± s.e.m.

Figure S7

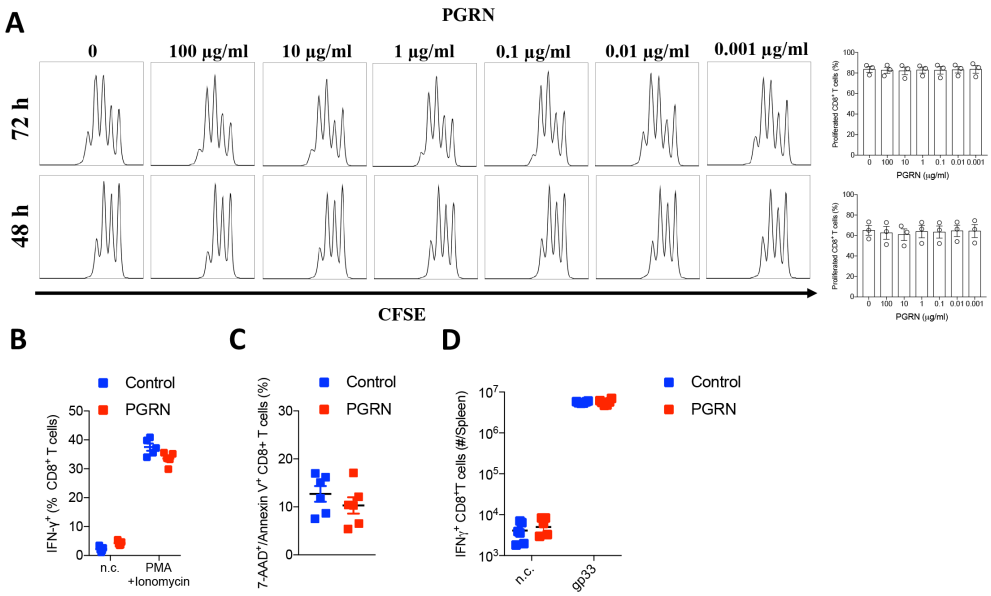

Supplementary Figure 7. PGRN does not limit CD8$^+$ T cell proliferation and activation. (A) Purified CD8$^+$ T cells were labelled with CFSE and then activated by anti-CD3/anti-CD28 antibodies and incubated with different doses of PGRN *in vitro*. The CFSE intensity was measured by flow cytometry at 48h and 72h (n=3). **(B)** Splenocytes from control mice were stimulated by PMA (20 ng/ml) and Ionomycin (1 µg/ml) for 6hours. Cells were subjected to IFN-γ staining (n=5). **(C)** Naïve CD8$^+$ T cells were activated with anti-CD3e/CD28 antibody with or without PGRN (100µg/ml) for 24h. The apoptosis of these T cells was measured by FACS (n=6). **(D)** Mice were infected with LCMV-WE. Splenocytes were re-stimulated with gp33 in absence and presence of PGRN (100 µg/ml) and IFN-γ in CD8$^+$ T cells was measured by FACS (n=6). Data show mean ± s.e.m.

Figure S8

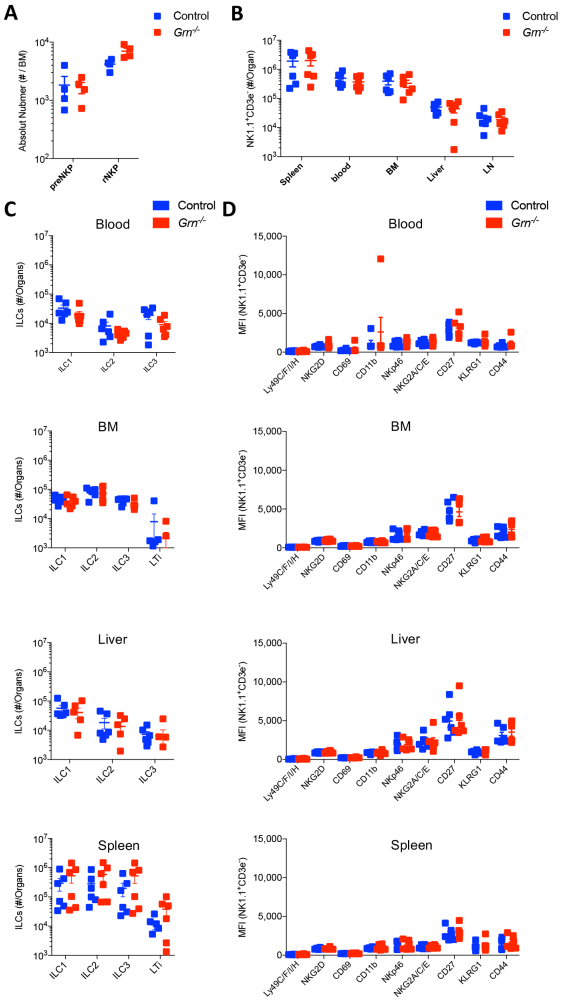

Supplementary Figure 8. *Grn*$^{-/-}$ mice exhibit no gross NK cell or Innate lymphoid cell phenotype. (A) Absolute numbers of NK cell progenitor preNKP (Lin$^-$2B4$^+$CD27$^+$CD127$^+$CD122$^-$Flt3$^-$) and rNKP (Lin$^-$2B4$^+$CD27$^+$CD127$^+$CD122$^+$Flt3$^-$) were measured by flow cytometry in bone marrow (BM) samples from control and *Grn*$^{-/-}$ mice (n=3). **(B)** CD3e$^-$NK1.1$^+$ cells in peripheral lymphoid organs were examined in *Grn*$^{-/-}$ and control mice (n=6). **(C)** ILC1 (Lin$^-$NK1.1$^+$RORγT$^-$ Eomes$^-$), ILC2 (Lin$^-$NK1.1$^-$RORγT$^-$CD11b$^-$GATA-3$^+$), ILC3 (Lin$^-$RORγT$^+$CD4$^-$) and LTi (Lin$^-$RORγT$^+$CD4$^+$) subsets were measured by flow cytometry in organs harvested from naive control and *Grn*$^{-/-}$ mice as indicated. Gating strategy excluded dead and Lin (CD3, CD5, CD8, CD19, Ly-6G, TCRβ, and FcγR1) cells (n=6). **(D)** Inhibitory and activating receptors of CD3e$^-$NK1.1$^+$ cells in the blood and peripheral lymphoid organs as indicated were examined in naive control and *Grn*$^{-/-}$ mice (n=6). Data show mean ± s.e.m.

Figure S9

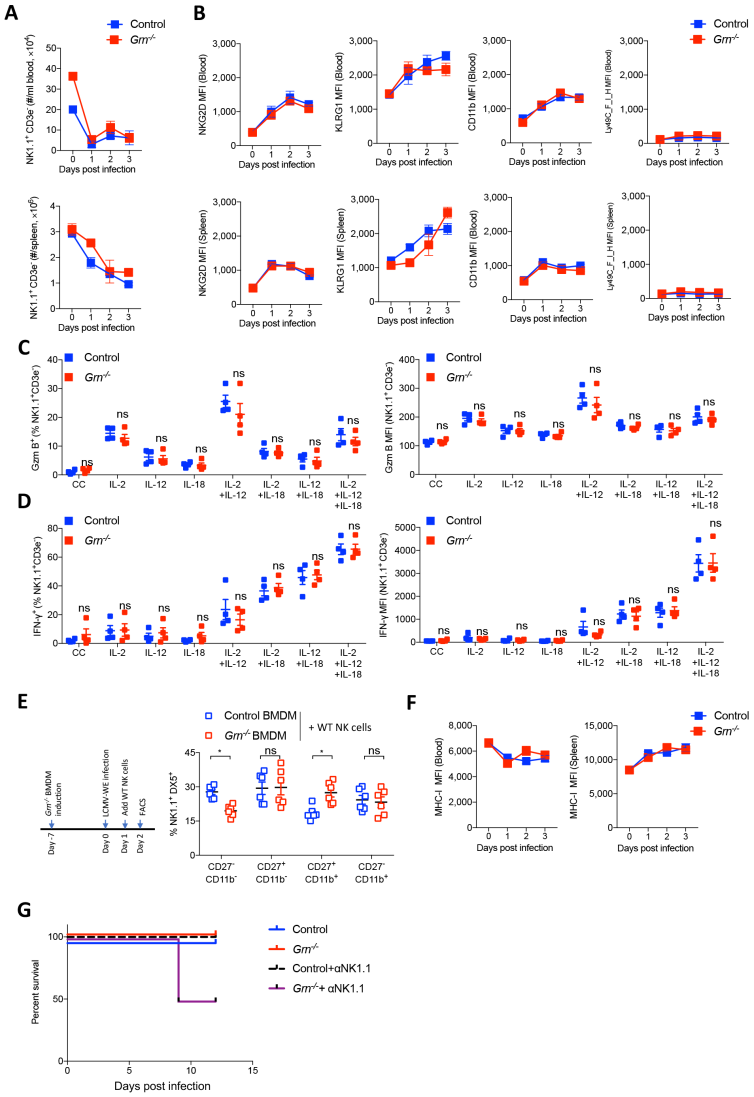

Supplementary Figure 9. *Grn*$^{-/-}$ mice exhibit similar NK cell numbers and surface molecule expression to control animals. **(A)** Control and *Grn*$^{-/-}$ mice were infected with 2x10^{6} pfu of LCMV-WE. Absolute numbers of CD3e^{-}NK1.1^{+} cells in blood (*upper panel*) and spleen (*lower panel*) samples were examined by flow cytometry (n=4). **(B)** Surface molecule expression was measured (n=4). **(C-D)** Control and *Grn*$^{-/-}$ splenocytes were activated with different cytokines as indicated for 6h. Gzm B **(C)** and IFN-γ **(D)** expression in NK cells was measured by flow cytometry (n=4). **(E)** Control and *Grn*$^{-/-}$ bone marrow derived macrophage (BMDM) were infected with LCMV (MOI=1) for 24h and isolated naïve WT NK cells were added to the culture. 24h later, NK cell

maturation was measured by flow cytometry (n=6). **(F)** WT and *Grn*$^{-/-}$ mice were infected with high dose of LCMV-WE. MHC-I expression on CD8^{+} T cells was measured by FACS (n=4). **(G)** WT and *Grn*$^{-/-}$ mice were injected with NK depletion antibody (αNK1.1) as shown in Figure 7D. The survival rate was measured (n=22). Data show mean ± s.e.m.; *ns* represents no significance, *$p < 0.05$, **$p < 0.001$.

Supplementary Table 1

Targets		Sequence (5'-3')
CDK9	Forward	GTACGACTCGGTGGAATGCC
	Reverse	GATGGGGAACCCCTCCTTCT
Cyclin T1	Forward	ATGCCTGATCGTACCGAGAAG
	Reverse	GTCGTTGGCGTAAATGAGCTG
Granzyme B	Forward	CCACTCTCGACCCTACATGG
	Reverse	GGCCCCCAAAGTGACATTTATT
Perforin	Forward	AGCACAAGTTCGTGCCAGG
	Reverse	GCGTCTCTCATTAGGGAGTTTTT
Grn	Forward	GTGTTGTGAGGATCACATTC
	Reverse	CTATGACCTTCTTCATCCAG
GAPDH	Forward	TGCACCACCAACTGCTTAG
	Reverse	GGATGCAGGGATGATGTTC
Actin	Forward	GGCTGTATTCCCCTCCATCG
	Reverse	CCAGTTGGTAACAATGCCATGT